Petrographic evidence of the past occurrence of gas hydrates in the Tertiary Piedmont Basin (NW Italy)

MARTIRE[1] L., NATALICCHIO[1] M., PETREA[1] C., CAVAGNA[1] S., CLARI[1] P., DELA PIERRE[1, 2] F.

PETROGRAPHIC EVIDENCE OF THE PAST OCCURRENCE OF GAS HYDRATES IN THE TERTIARY PIEDMONT BASIN (NW ITALY).

[1] Dipartimento di Scienze della Terra, University of Torino, Italy

[2] CNR, Istituto di Geoscienze e Georisorse, sezione di Torino, Italy

Corresponding author: MARTIRE Luca

Email: luca.martire@unito.it tel. 39-011-6705194 fax 39-011-6705339

ABSTRACT

Methane-derived rocks in Monferrato and the Tertiary Piedmont Basin consist of seep carbonates, formed by gas seepage at the sea floor, and macroconcretions, resulting from cementation of buried sediments crossed by gas-rich fluids. These rocks are characterized by both negative $\delta^{13}C$ values and a marked enrichment in ^{18}O. Petrographic features that are not commonly described and that point to unconventional depositional and diagenetic conditions have been observed in both types of rocks: inhomogeneous distribution of cements within cavities; dolomite crystals floating within a cavity-filling calcite spar; non-gravitational fabrics of internal sediments plastering cavity walls; open framework within microbial crusts. These features suggest the former presence of gas hydrates in sediments. During their dissociation, new space was formed and filled with authigenic carbonates or injected sediments. The fabrics of gas hydrates and the geochemical conditions of sediments, in turn depending on the relative rates of supply of methane-rich fluids and normal seawaters, conditioned the final aspect of the rocks.

Keywords: methane-derived carbonates, gas hydrates, clathrites, Tertiary Piedmont Basin.

Introduction

Gas hydrates are ice-like crystalline compounds of water and gas whose stability depends on temperature, pressure and availability of gas and water (e.g. Kvenvolden 1998; Beauchamp 2004). Variations of these parameters, due to different processes such as sea level drop, tectonic uplift, temperature changes, can induce the destabilization of hydrates. In the last decade, a lot of research has been made on methane hydrates for three main reasons: gas hydrates are an important potential energy resource (e.g. Collet 2002; Milkov 2004); methane is an effective greenhouse gas (e.g. Dickens 2003); the sudden release of huge amounts of gas, delivered by gas hydrate dissociation, may trigger large scale landslides on continental margins (e.g. Haq 1993; Mienert 1998, 2005; Paull et al. 1996).

Gas hydrates have been directly observed or even sampled on present day sea floors and are clearly imaged on seismic profiles as bottom simulating reflectors (Pecher et al. 2001, Sain et al. 2000). Much less, however, is known about the past occurrence of gas hydrates in stratigraphic successions exposed on land (Pierre et al. 2002).

Anaerobic oxidation of methane (AOM), accomplished by consortia of methane oxidizing archaea and sulphate reducing bacteria, is a well known process leading to abundant calcite, aragonite and/or dolomite precipitation (e.g. Boetius et al. 2000; Meister et al., 2007, 2008); authigenic carbonates have actually been described to form within or in proximity to gas hydrates (e.g. Greinert et al. 2001; Teichert et al. 2005; Mazzini et al. 2006) and have been recently named clathrites (Bohrmann et al. 2002). Because of the isotope fractionation inherent with gas hydrate formation, the $\delta\ ^{18}O$ signature of these carbonates allows to relate them to gas hydrate. In particular, negative $\delta\ ^{18}O$ values may be associated to gas hydrate formation whereas positive values are related to dissociation events (e.g. Aloisi et al. 2000; Clari et al. 2004; Pierre and Rouchy 2004). Therefore the O isotope signature of fossil CH_4-derived carbonates is the only means so far available to infer a possible role of gas hydrates in their genesis, even though other mechanisms, such as illitization of smectite, can also be called upon to explain the ^{18}O fractionation (Dählmann and de Lange 2003). Clathrites, however, have only been described macroscopically whereas detailed microscopic observations have not been published and illustrated.

CH_4-derived rocks have been known for a long time in the Tertiary Piedmont Basin (Clari et al. 1988) where they occur in several places scattered over a very wide area (Fig. 1), as carbonate-rich masses of various size (dm3 to hm3) at different stratigraphic levels. Given the richness of examples, these rocks have been recently reanalysed, in the light of the current state of knowledge concerning seeps and gas hydrates in modern continental margins, with the purpose of looking for the possible evidence of the past occurrence of hydrates in these rocks. In particular it has been pointed out that gas hydrates are not always massive but may show porous fabrics (e.g. Bohrmann and Torres 2006) that the gas hydrate stability zone is not an impermeable barrier but it can be crossed by gas-charged fluids, and that gas hydrate dissociation may proceed at the same level side by side with gas hydrate formation (e.g. Liu and Flemings, 2006). In such settings, AOM can trigger precipitation of authigenic carbonates within primary pores of the gas hydrates and/or in new pores that are progressively generated by gas hydrate dissociation. It may be envisioned that these carbonate cements precipitating along with hydrate dissociation should be characterized by geometries and distributions that contrast with what commonly seen in cements growing in pores simply filled with porewaters, The purpose of this paper is to describe unusual petrographic features that could be referred to this process. These structures have only scantily been reported in literature, and would stand as one of the first direct evidence of a fossil gas hydrate stability zone (GHSZ) in ancient sedimentary successions.

Materials and methods

The studied methane-derived carbonate-rich rocks have been first observed and described in outcrop, with particular attention to the geometry of the lithified bodies and to the relationships with the hosting sediments. Hundreds of samples have been collected through the years and several tens of thin sections prepared from selected specimens. Petrographic studies were carried out by plane and cross polarized light microscopy and with the aid of cathodoluminescence using a CITL 8220 MK3 equipment (working conditions: about 17kV and 400 μA). Carbonate (calcite, dolomite, aragonite) and non-carbonate phases (pyrite, silicates) were identified by means of an EDS microprobe Link System connected to a scanning electron microscope (Cambridge S-360). SEM morphological observations were performed on both broken chips and slightly etched polished surfaces. Thin sections were analysed further for their UV-fluorescence, to reveal occurrence and distribution of organic matter, by using ultraviolet light (illumination source 450-490 nm) performed with a Nikon microscope with a UV-2A filter block. Tens of samples have also been prepared for C and O stable isotope analyses: the carbonate fraction has been analysed following the classical method (Mc Crea 1950), according to which carbonate powder reacts in vacuum conditions with 99% orthophosphoric acid at 25°C (time of reaction: 4 hours for calcite and 7 hours for dolomite). The $^{13}C/^{12}C$ and $^{18}O/^{16}O$ ratios of the CO_2 obtained were analysed by means of a Finnigan MAT 250 mass spectrometer. The isotopic ratios are expressed as $\delta\,^{13}C$ and $\delta\,^{18}O$ per mil versus the PDB standard; the analytical error is ±0.5‰ and ±0.1‰ for $\delta\,^{13}C$ and $\delta\,^{18}O$, respectively.

Geological setting

The Tertiary Piedmont Basin is composed of upper Eocene to Messinian sediments deposited unconformably, after the mesoalpine collisional event, on both alpine metamorphic rocks and Apennine Ligurian units (e.g. Gelati and Gnaccolini 1988; Castellarin 1994; Mutti et al. 1995; Roure et al. 1996). Deposition of these sediments was strongly influenced by synsedimentary compressional tectonics, related to the building of the Apennine thrust belt. As a consequence, several tectono-sedimentary domains (the Tertiary Piedmont Basin s.s. to the South, and the Monferrato and Torino Hill to the North), resting on different crustal blocks and characterized by different sedimentary features, developed during the Cenozoic (Clari et al. 1995; Piana and Polino 1995). Although the relationships among these domains are masked by Pliocene to Quaternary deposits (Fig. 1) seismic profiles show that their boundaries correspond to long-lived, major tectonic structures (e.g. Biella et al. 1997).

Both the Tertiary Piedmont Basin s.s. and the Monferrato – Torino Hill are overthrusted to the North onto the Po Plain foredeep, along the late Neogene to Quaternary Padane thrust fronts (Fig. 1), presently buried below the Quaternary Po plain deposits (Castellarin 1994; Falletti et al. 1995; Dalla et al. 1992).

The studied samples have been collected both in Monferrato and in the eastern sector of the Tertiary Piedmont Basin, in the Ripa dello Zolfo area. The stratigraphic setting of these two sectors is briefly illustrated below (For a detailed stratigraphic setting of the studied localities, see Clari et al., 2009; Dela Pierre et al., 2009).

Monferrato

The Monferrato stratigraphic succession ranges in age from Late Eocene to Late Miocene (Messinian) and mainly consists of terrigenous sediments that unconformably overlie Mesozoic mélanges (Ligurian units) originated in the Alpine accretionary prism (e.g. Pini 1999). Deposition of Oligocene and Lower Miocene sediments was controlled by a complex sea floor topography produced by NW-SE-trending transpressive faults (Clari et al. 1995; Piana and Polino 1995; Piana 2000). The thickest successions consist of fine grained deep water facies deposited in fault-bounded subbasins. On intervening structural highs (e.g. the Marmorito and Villadeati - Alfiano Natta paleohighs, where the

studied samples were collected), coarse fan delta sediments were deposited. These sites are also characterized by the occurrence of erosional unconformities and extensive hiatuses (e.g. the Oligocene-Messinian boundary of the Villadeati-Alfiano Natta paleo-high: Clari et al. 1995; Dela Pierre et al. 2003). Middle to Upper Miocene sediments consist of outer shelf to slope fine-grained sediments of Langhian - Tortonian age that are unconformably overlain by an Upper Messinian mélange (Valle Versa chaotic complex: Dela Pierre et al. 2002, 2003) that is made up of blocks of different nature (Ca sulfates and a wide range of carbonate facies) floating in a fine grained matrix.

Ripa dello Zolfo

The Ripa dello Zolfo area is located in the eastern part of the Tertiary Piedmont Basin (Fig. 1), south of the Villalvernia-Varzi Line, a E-W striking strike-slip fault that was considered as the Alps-Apennine boundary (Elter and Pertusati 1973).

The stratigraphic succession exposed here ranges in age from Oligocene to Messinian and unconformably overlies Ligurian Cretaceous turbidites (Ghibaudo et al. 1985). It starts with coarse grained Oligocene shallow water sediments, followed by upper Oligocene to Middle Miocene deep water facies.

The Upper Miocene part of the succession consists of Tortonian - lower Messinian fine-grained outer shelf to slope sediments (Sant'Agata Fossili Marls) that are unconformably overlain by the Valle Versa chaotic complex (upper Messinian). The latter is in turn followed by brackish water deposits known as Conglomerati di Cassano Spinola (upper Messinian).

The Sant'Agata Fossili Marls, that host the studied samples, consists of two members (Clari and Ghibaudo 1979):
- the lower member (Tortonian), about 180 m thick, is made up of outer shelf sandstones and muddy siltstones (Ghibaudo et al. 1985). At its top, several multiple intraformational discordances**,** corresponding to slump scars, occur (Clari and Ghibaudo 1979);
- the upper member (lower Messinian) is about 80 m thick and consists of homogeneous blue-grey silty marls with thin bedded turbidites, indicative of a slope depositional environment (Ghibaudo et al. 1985).

This vertical evolution is related to the deepening of the basin, interpreted to be of tectonic origin, as suggested by the occurrence of slump scars resulting from oversteepening of a gentle slope and consequent downslope sliding of variably thick sediment packages (Ghibaudo et al. 1985).

The Tertiary Piedmont Basin clathrites

The present research was focussed on three selected outcrops, two in Monferrato (Marmorito and Alfiano Natta) and one in the eastern sector of the Tertiary Piedmont Basin (Ripa dello Zolfo)(Fig. 1). Monferrato is one of the first places in the world where the fossil products of CH_4-rich fluid seepage were identified (Clari et al. 1988). Recent developments of research in this area and the discovery of new outcrops in the eastern sector of the Tertiary Piedmont Basin allowed to distinguish two types of methane-derived rocks: 1) macroconcretions, generated by localized precipitation of carbonate cements within the pores of buried sediments located at variable depths below the sea floor and along the upward flow path of gas-rich fluids, and 2) seep carbonates, formed by expulsion of gas-rich fluids at the sea floor (Clari et al. 2009). Both these types of rocks are characterized by negative $\delta^{13}C$ values (up to -52‰ PDB) and, especially the macroconcretions, systematically positive $\delta^{18}O$ values (up to + 7 ‰ PDB) (for summary of isotopic data see Clari et al. 2009).

Monferrato

At Alfiano Natta and Marmorito, macroconcretions form variably large indurated masses, up to 100.000's of m^3. They are developed within fan delta deposits consisting of interbedded conglomerates, sandstones and mudrocks of Oligocene and Aquitanian age respectively. At Marmorito, they grade upward to lower Burdigalian diatomites in turn followed by poorly exposed thin Messinian siltites. At Alfiano Natta, instead, they are overlain unconformably by upper Messinian chaotic deposits (Valle Versa Chaotic Complex, Dela Pierre et al. 2002, 2007). The strong induration of macroconcretion is due to the presence of an abundant intergranular dolomite cement. A striking feature of the macroconcretions is the presence of a pervasive network of mainly subvertical clastic dykes and veins. Dykes vary from millimeters to some decimeters in width and are filled with a variety of sediments ranging from mudstones to sandstones; brecciated textures result from polyphase opening of the same fracture. Veins show complex carbonate cement infillings with a variety of mineralogies (aragonite, calcite, dolomite) and morphologies (fibrous, sparry, peloidal). These macroconcretions are inferred to have developed during Messinian deformation and massive fluid expulsion through older sediments (Clari et al. 2009).

In the surroundings of Marmorito, typical seep carbonates (*Lucina* Limestone), consisting of cream coloured marly limestones and characterized by a variably dense packing of chemosynthetic bivalves (*Lucina*), have also been reported (Clari et al. 1988, 1994). They are commonly found as ex situ blocks scattered at the base of present day slopes. The recent finding of a in situ seep carbonate mass within silty outer shelf marls allows to date this seepage event, less widespread and effective than the Messinian one, to the Langhian (Clari et al. 2009).

Ripa dello Zolfo

Different methane-derived carbonate-rich rocks, including Lucina limestones and concretions, occur at Ripa dello Zolfo, in the eastern sector of the Tertiary Piedmont Basin, within the upper member of the Sant'Agata Fossili marls (lower Messinian) that consists of silty slope marls (Ghibaudo et al. 1985; Dela Pierre et al., 2009). A variety of concretions has been observed, among which bed-parallel ones showing a thickness up to 50 cm and a lateral extent of some tens of metres. In these concretions no remains of chemosynthetic organisms, such as lucinoid bivalves or tube worms, and evidence of sea-floor exposure occur. A Messinian phase of gas-rich fluid expulsion is inferred also for these concretions (Dela Pierre et al., 2009).

Microstructures

In all methane-derived rocks of Monferrato and Ripa dello Zolfo, enigmatic features that cannot be explained with common knowledge of sedimentary petrology and in our opinion suggest the former presence of gas hydrates, commonly occur. Some selected examples will be described below and an interpretation proposed.

1. Pinch outs of fringing cements

These structures have been observed in typical seep *Lucina* limestones, at Marmorito in Monferrato, that show $\delta^{13}C$ values from -25 to -35‰ PDB) and $\delta^{18}O$ values from +0.1 to + 0.9 ‰ PDB. A common feature is the presence of irregular cavities, with rounded edges and up to 2 cm wide, filled with cements (Fig. 2). These cavities are interpreted as fluid conduits, most probably following former burrows, developed within semilithifed fine-grained sediments in close proximity to the sea bottom (Clari & Martire, 2000). Some grains, such as faecal pellets, may also be present on the cavity floor. The filling cements are mainly represented by aragonite and inclusion-rich calcite, but microsparitic and coarse limpid sparry calcite also occur. Even though a typical centripetal growth of subsequent cement layers

predominates, notable exceptions are common that are due to marked differences in the distribution of the first cement generations that only coat a part of the cavity and abruptly stop against the cavity walls (Fig. 2). The following generations, instead, centripetally and isopachously fill the remaining void.

An even clearer example of this fabric has been observed in the bed-parallel concretions at Ripa dello Zolfo, in the eastern sector of the Tertiary Piedmont Basin (for more details see Dela Pierre et al., 2009). These concretions are indurated due to a very finely crystalline intergranular dolomite cement ($\delta^{13}C$ -25 to -34‰ PDB; $\delta^{18}O$ +6.0 to +7.0 ‰ PDB) show a more or less complex network of mainly bed parallel fractures, commonly wedge-shaped, mm- to some cm-wide, that, from the core of the concretion, gradually thin outward, giving rise to features that strongly recall septarian cracks. Syneresis seems the most probable cause of fissure opening,. This process is held to be responsible for the opening of contractional cracks in muddy sediments, especially where it is enhanced by the decay of bacterial extracellular polysaccharide substances (EPS) (e.g., Dewhurst et al., 1999; Hendry et al., 2006). Some of these wedge-shaped fractures are empty, others are filled either with internal sediments or carbonate cements. The latter consist of sparry dolomite and calcite ($\delta^{13}C$ -28 to -43‰ PDB; $\delta^{18}O$ -5.0 to +6.0 ‰ PDB) and show a banding defined by the alternance of turbid and limpid layers (Fig. 3a). Cathodoluminescence helps to highlight the great complexity in the distribution of these cements (Fig. 3b). A first thin rim of dull to bright yellow dolomite fringes the crack walls isopachously (cement 1 in Fig. 3c). It is followed by a dull brown to moderate orange zoned calcite cement that does not overgrow uniformly the first dolomite rim. In particular, the first dull brown zone (cement 2 in Fig. 3c) shows marked variations in thickness and even tapers out completely. Consequently the next, orange luminescing, cement zone in some portions of the fracture walls directly overlies the first isopachous dolomite rim (cement 3 in Fig. 3c). Because of this strongly inhomogeneous distribution of cement zones, two adjacent fractures may show markedly different fillings, one being almost fully plugged with the dull brown zone that, instead, is nearly absent in the other (Fig. 3b). By analogy with the terminology used in lithostratigraphy for bed terminations, this feature will be hereafter referred to as cement pinch out.

2. Non gravitational fabrics in cavity fills

In the *Lucina* limestones of Marmorito, other cavities, even larger than those described in the previous paragraph, are mainly filled with fine-grained carbonates (Fig. 4a). These internal sediments range from micrite to silt-sized pelsparites that show a loose packing and also include scattered planktonic foraminifer tests and siliciclastic grains (Fig. 4b). They are also locally characterized by an irregular lamination defined by alternation of finer and coarser laminae (Fig. 4c). Three enigmatic features characterize such sediments: some pelsparitic laminae are separated from the next by calcite sparry cement; sediments not only cover the cavity floor but are plastered also on the lateral walls and the ceiling of the cavity so that single laminae may be followed all around the cavity edges (Fig. 4c); where the distribution of internal sediments is discontinuous, the same sediment is observed to occur on the bottom or "stuck" to a vertical wall, and sediment and sparry cement patches are very irregularly juxtaposed (Fig. 4a). These fabrics represent incongruent geopetal structures within a single cavity and document infilling mechanisms not governed by gravity.

3. Dolomite crystals floating in void-filling coarse calcite spar

The Marmorito macroconcretion is crossed by a network of mainly subvertical sediment-filled dykes and cement-filled veins (Fig. 5a). Some of these are some centimetres large and show particularly complex infillings. The walls of the veins, occurring within dolomite-cemented sandstones, are rimmed by a finely crystalline to microcrystalline luminescent dolomite organized in fine laminae that follow the shape of the fracture walls. This rim,

about 0.5 mm thick, is overlain basically by a non-drusy mosaic of equant coarse sparry calcite cement with a undulous extinction ($\delta^{13}C$ -27 to -28‰ PDB; $\delta^{18}O$ +3.4 to +3.5 ‰ PDB). It is moderate orange in CL and shows a complex sectorial zoning. Poikilotopically engulfed by this coarse calcite spar, zoned dolomite is easily recognized due to its greenish yellow to brown luminescence (Figs. 5b, c, d). It occurs as euhedral rhombic crystals and as sphaerulites up to 200 μm across, scattered or mainly clustered in patches up to a few mm across ($\delta^{13}C$ -35 to -40‰ PDB; $\delta^{18}O$ +3.0 to +4.7 ‰ PDB). Sphaerulites commonly have hollow cores that may show dumbbell shapes. Although the latter have also been obtained abiotically (Fernandez Diaz et al., 1996; Tracy et al., 1998; Warren et al., 2001), dumbbell shapes are commonly reported in bacterially induced carbonate precipitates (e.g. Buczynski & Chafetz, 1991; Brehm et al., 2006; Chekroun et al., 2004). A marked greenish-yellow fluorescence, that contrasts with the very weak one of the surrounding calcite spar (Fig. 5e), shows the presence of organic matter within the authigenic carbonate and thus supports a microbial origin already presented previously (Cavagna et al. 1999; Clari and Martire 2000). The central part of many dolomite rhombs and sphaerulites moreover is irregularly occupied by the orange calcite spar.

4. Open framework structures in microbial mats

The Alfiano Natta macroconcretion is crossed by a network of fractures that are larger, denser and more complex than those of Marmorito. The complete description of their filling is out of the scopes of this paper. The attention here is focussed on a feature that is locally observed. Some fractures, about 10 cm large, show encrustation by authigenic carbonates on the walls and injected sediment infill in the centre. The authigenic carbonates show a wide variety of mineralogies and growth morphologies and also include thin microcrystalline laminated crusts (Fig. 6a). The laminae (about 30 μm thick) tightly overlie each other and follow the micromorphology of the substrate they coat (Fig. 6b). The overall "stromatolitic" aspect of these crusts recalls calcified bacterial mats and the bright epifluorescence of the single laminae confirm the fundamental contribution of microbial communities in their genesis (Fig. 6c). Commonly, however, the laminae divert and are widely spaced giving rise to an irregular fenestral fabric, with fenestrae up to a few millimetres large. Some fenestrae are very smooth and ellipsoidal, others are quite irregular and show a sort of internal subdivision due to the inward branching of single microcrystalline laminae that surround them (Fig. 6a). The fenestrae are filled with a dolomite and calcite crystal mosaic zoned in CL (Figs. 6d, e). These cements are partly turbid and partly limpid; the turbid parts occur both as discontinuous rims and as isolated patches and commonly preserve ghosts of a fibrous fabric clearly due to aragonite recrystallization (Fig. 6f). All these carbonates show negative C isotopes and quite positive O isotopes ($\delta^{13}C$ -17.0 to -21.9 ‰ PDB; $\delta^{18}O$ -+1.9.0 to +5.9 ‰ PDB).

5. Geopetal fill of moldic cavities of former clasts

In the Alfiano Natta macroconcretion, some dykes consist of grain-supported coarse muddy sandstones in which no cement-filled pores are recognizable because of the abundance of the muddy matrix (Fig. 7a). The rock is lithified by a finely crystalline dolomite grown in the pores of the matrix ($\delta^{13}C$ -16.2 to -22.3 ‰ PDB; $\delta^{18}O$ +5.0 to +6.0 ‰ PDB). In cathodoluminescence this dolomite is zoned and ranges from orange to brown. Clastic grains of the sandstone are made up of serpentinite, quartz, K feldspars, plagioclase and lithic fragments of Mesozoic micritic limestones. In addition to these, other carbonate grains, angular to subrounded in shape, 0.5 to 1.0 mm across, also occur. Some of them show an internal complexity due to the presence of both a fine-grained sediment, also containing framboidal pyrite, cemented by finely crystalline dolomite (crystals 10 to 30 μm), and of limpid coarser sparry dolomite (crystals up to 400 μm), locally showing a drusy fabric (Figs. 7b, c, d); commonly a hollow core is also present. The finely crystalline dolomite systematically occurs in the lower part, and the coarse dolomite in the upper one, giving rise to

typical geopetal structures. Cathodoluminescence shows that a first generation of brightly luminescing dolomite nucleated as scattered crystals in the sediment and formed a thin rim growing inward from the outer edge (Fig. 7c). It is overgrown by a moderately luminescing brown zone (II), and a very dull brown zone (III) that is only met in the limpid coarse dolomite. These features indicate that these are not primary clastic grains but moldic secondary pores generated by dissolution and later filled in a rather complex way.

Other carbonate grains also occur which are completely composed of the finely crystalline dolomite mosaic, identical in size and CL zoning to the lower part of the geopetally-filled moldic pores (Figs. 7e, f).

Discussion

All the described diagenetic fabrics, despite marked differences, share a common feature i.e. they all deviate from basic rules in sedimentary petrology. This deviation may be in two opposite ways: a) In some cases it is not found what should be there. For example, irregular layers of pinching out cements (Fig. 3) occurring on the walls of cavities indicate that something hindered formation of what should form in a water-filled void i.e. uniform rims of isopachous cements. b) In other instances, in contrast, it is found what should not be there: dolomite crystals grown in the middle of a cavity subsequently plugged by calcite spar i.e. in the apparent absence of a substrate (Fig. 5); laminated sediments plastering cavity walls instead of gravitationally accumulate on the bottom (Fig. 4). The most likely process which could explain all these fabrics, as well as the geopetal fill of moldic cavities in sandstone dykes, is dissolution of a metastable phase that fully or partly occupied the cavities; this phase represented a solid substrate that could be coated by microbial communities or encrusted by authigenic carbonates, and then was dissolved, leaving voids of various size and shape. The geometry of these voids is not consistent with any of the growth morphologies of easily dissolvable carbonates such as aragonite or Mg-calcite. Taking into consideration that, on the basis of the isotope data presented, the carbonate fraction of the rocks in which these fabric are found is all methane-derived, we hypothesize that the metastable phase could correspond to gas hydrate. The systematically positive or strongly positive $\delta^{18}O$ values of the authigenic carbonates contribute to support this hypothesis.

In this light, each of the described features may be explained in a relatively simple way by calling upon the same basic process related to formation and dissociation of gas hydrates.

1) Pinching out cements grew in cavities during dissociation of gas hydrates that previously fully occupied them. Dissociation started from the walls of the voids and proceeded centripetally at relatively slow rates (Fig. 8). This allowed carbonate precipitation to take place concomitantly with gas hydrate dissociation, at every step filling the newly generated free spaces that extended from the cavity walls and the external surface of the still stable gas hydrate mass. Slightly changing geochemical conditions are recorded by different cathodoluminescence colours of the authigenic carbonates. A possible alternative for the genesis of the Ripa dello Zolfo pinching out cements could be cementation during progressive opening of tectonic cracks. This hypothesis has been ruled out for two main reasones: 1) tectonic features, not ubiquitously recognizable, are represented by dm-spaced cleavages that cross all the beds and show a typical rheologically controlled refraction, from subvertical in more cemented layers to more gently sloping in the marls and thus are clearly distinguishable from the irregular, but mainly subhorizontal, wedge-shaped, septarian-like, cracks hosting the pinch out cements; 2) the cracks are lined by the isopachous rim of brightly luminescing cement 1; should the cracks have opened by successive steps, the first cement crust would have been broken and the fragments fallen down on the floor of the fissure. A tectonic origin, moreover, cannot be applied for the Monferrato pinching out cements that grow within small, rounded cavities interpreted as fluid conduits.

2) Non-gravitational fabrics, displayed by internal sediments partially filling cavities, record the disappearance of gas hydrates plugging fluid conduits, each step of progressive dissociation being followed by the reactivation of flow of fluids entraining fine-grained sediments and triggering carbonate precipitation both as microbially-induced microcrystalline calcite or dolomite at the hydrate surface or even within it, and as intergranular sparry cement (Fig. 9). Different patterns of dissociation, random vs. more or less regularly centripetal, resulted in non-continuous patches of internal sediments or relatively continuous laminated sediments parallel to cavity walls respectively.

3) As to the dolomite crystals floating in calcite spar, some points can be stated:

- Dolomite rhombs and sphaerulites, limpid and subtly zoned in CL, clearly precede the coarse calcite spar in which are poikilotopically engulfed.
- Dolomite rhombs and sphaerulites, especially at the first stages of growth did not form a self-supporting framework and thus could not develop and "float" in an empty cavity in the absence of a solid substrate
- No relics or ghosts of a carbonate precursor are observable in the orange luminescing, limpid calcite spar even if aragonite precipitation and subsequent dissolution are frequently observed in Monferrato CH_4-derived carbonates (Clari and Martire 1995, Clari et al. 2009).This allows to rule out that the solid substrate necessary to sustain the rhombs and spherulites could be a former aragonite cement. subsequently dissolved.

On the basis of these considerations, the following evolution may be sketched (Fig. 10). Fractures opened within dolomite-cemented sandstones and were at first lined by microbial mats that promoted precipitation of microcrystalline laminated carbonates. Gas hydrates, locally characterized by a fine bubble fabric, plugged the open spaces. When they started to dissociate, dolomite precipitated around coccoidal microbial colonies within the hydrate pores. Coarse calcite spar at last precipitated in all the open spaces after complete disappearance of gas hydrates. The scarcity of CL concentrical zoning of these cements could suggest a rather rapid precipitation, i.e. in relatively stable geochemical conditions.

4) Open framework structures, similar to those described above, have also been reported in literature as primary voids within microbial carbonates. They are mainly related to light-dependant cyanobacteria both inferred in ancient submarine environments affected by methane seepage and stromatolite-like growth (Gomez Perez 2003), and observed in modern travertines found at thermal springs (Arp et al. 1998, Pache et al. 2001). In the latters, dehydration and shrinkage of the organic mucus (Extracellular Polymeric Substance) of the microbial mats and development of gas bubbles resulted in formation of irregular and lenticular voids. Even though the role of this mechanism cannot be ruled out, the general context (fractures occurring within lithified sediments at a certain depth below the sea floor) and the positive $\delta^{18}O$ values of the authigenic carbonates lead to consider another mechanism.

The geometry of the fenestral fabrics in microbial mats strongly and directly recalls the vacuolar structure displayed by some gas hydrates recovered from present day continental margins (Bohrmann et al. 1998; Bohrmann and Torres 2006; Mazzini et al. 2006). It is thus possible to envisage that gas hydrates, grown in a fracture, at least locally showed a vacuolar fabric that could allow gas-rich fluids to flow through it (Fig. 11). The hollows were then filled with aragonite. Dissociation of gas hydrates then started and proceeded at a slow rate. Concomitantly, authigenic carbonates precipitated, as microcrystalline crusts, at the gas hydrate retreating surface and around the aragonite-filled former vacuoles insofar replacing their delicate wall and permanently recording the 3D framework. Aragonite was then partially dissolved, the relics recrystallized to calcite or dolomite preserving ghosts of the pristine fibrous habit, and the voids filled with zoned sparry calcite and dolomite. The result is a complex crust with irregularly laminated microcrystalline carbonate replacing gas hydrate, and sparry calcite and dolomite forming molds of hydrate vacuoles.

5) At last, the geopetally filled moldic cavities cannot be due to dissolution of labile grains such as feldspars, plagioclase and clastic carbonates that are perfectly preserved in these rocks; also aragonite clasts are excluded because the rounded edges cannot be reconciled with the fibrous habit of aragonite that would generate very irregular, spiky margins as observed in other dykes at Alfiano Natta. The geopetally filled moldic cavities in contrast may be interpreted as small clasts of almost pure gas hydrates (Fig. 12). They were formed within clastic dykes, disrupted and transported upwards by a new phase of violent fluid and sediment injection. When gas hydrate started to dissociate, a void was essentially left: clay particles, previously floating in the clathrate, fell down upon gas hydrate disappearance under the action of gravity and gave rise to geopetal structures. Framboidal pyrite and brightly luminescing finely crystalline dolomite, both related to anaerobic oxidation of methane, formed within this sediment flooring the moldic pore; luminescing dolomite also rimmed the cavity walls. Coarser sparry dolomite, at last, almost completely plugged the remaining void. The fine-grained dolomite clasts may instead be interpreted as small clasts of clathrate-cemented muds. Dissociation of gas hydrates left mud clasts with a high porosity within which the same brightly luminescing finely crystalline dolomite occurring in the geopetal moldic cavities could nucleate.

The described diagenetic fabrics, moreover, could also allow to infer different pristine fabrics of gas hydrates. Pinching out cements and non-gravitational internal sediments likely formed within cavities plugged by massive gas hydrates, whereas open frameworks in microbial mats and floating dolomite spherulites record carbonate precipitation within gas hydrates characterized by a bubble fabric. Most of the described anomalous features result from the generation of cavities during gas hydrate dissociation and concomitant filling by carbonate cements of various aspects and mineralogy. By paraphrasing the polyphase mechanism of tectonic vein filling, named crack-seal (Ramsay 1980), we propose to use the term melt-seal for this new kind of diagenetic sedimentary structure. The zebra and stromatactis structures, related to clathrate freeze-and-thaw processes by Krause (2001), and the carbonate breccias interpreted by Bojanowski (2007) as due to cementation and then replacement of gas hydrate clasts, are further examples, not met in the Tertiary Piedmont Basin, that perfectly falls within this category.

Conclusions

The described fabrics of methane-derived authigenic carbonates of the Tertiary Piedmont Basin are particularly complex and point to processes that cannot be unravelled in the light of the common knowledge in sedimentary petrology. They are here interpreted as the result of carbonate precipitation in the open spaces left by gas hydrate destabilization and, because of this, named melt-seal structures. The recognition of these features provides the only direct evidence so far available of the past occurrence of gas hydrates in ancient sediments and hence of a fossil gas hydrate stability zone.

Although the genetic process proposed is the same for all the described examples, i.e. formation and dissociation of clathrates, markedly different structures result. This may be related to the interplay of some factors: 1) the original fabric of gas hydrates that can be massive or vacuolar; 2) rates and modes of dissociation of gas hydrates; a rapid dissociation generated open spaces that were filled by authigenic carbonates in a simple, non-diagnostic way (e.g. calcite spar engulfing dolomite sphaerulites), whereas a progressive dissociation proceeding along with carbonate precipitation produced melt-seal diagnostic features (e.g. pinching out cements, discontinuous internal sediments); 3) biogeochemical conditions constraining mineralogy and growth morphologies of authigenic carbonates; in particular, the degree of supersaturation and the concentration of sulfates are considered to favour aragonite precipitation over Mg-bearing carbonates (e.g. Reitner et al. 2005). The chemistry of pore fluids within buried sediments, in turn, obviously strictly depends on the balance between the continuous downward supply of seawaters, containing sulfate, and the

upward flux of methane-rich fluids. The described Tertiary Piedmont Basin clathrites therefore document a relatively shallow gas hydrate stability zone, i.e. in the reach of a downward advection of normal sea waters, as recently observed during periods of active seepage in present day settings (Solomon et al. 2008).

A re-examination of sediments hosting methane-derived authigenic carbonates, carried out in the light of this working hypothesis, could on one side widen the spectrum of melt-and-seal fabrics and on the other side contribute to better understand aspects, such as the behaviour and evolution of gas hydrates and of the hosting sediments, that cannot be properly addressed in a time perspective in present sea floor exploration.

Captions of figures

Fig.1 – Structural sketch map of NW Italy (modified from Bigi et al., 1990) and location of the studied sections. (1: Marmorito; 2: Alfiano Natta; 3: Ripa dello Zolfo. TPB:Teriary Piedmont Basin; PTF: Padane Thrust Front; VVL: Villalvernia Varzi Line).

Fig.2 – Marmorito, *Lucina* Limestone. Cross section of a fluid conduit likely developed on a burrow. Except for a few faecal pellets in the centre bottom, it is completely filled with cements. The first generations do not encrust all the cavity walls but stop abruptly against them (arrows). Thin section.

Fig.3 – Ripa dello Zolfo, Marne di S.Agata Fossili. a, b) Transmitted light and cathodoluminescence picture of a bed parallel cement-filled fissure c) Simplified line drawing evidencing the main generations of cements (1 to 4:oldest to youngest) and their inhomogeneous thickness and distribution. Thin section.

Fig.4 - Marmorito, *Lucina* Limestone. a) Sediment- and cement-filled cavity. Note the distribution of sediments and cements at the bottom of the cavity and on the right side, that give rise to two incongruent geopetal structures in the same cavity. b) Close up of Fig. 4a. Note the loose packing of peloids and the presence of scattered clastic grains (foraminifer test encircled). Thin section. c) Laminated, peloidal to micritic sediments partially infilling a cavity. Note that some laminae may be followed from the floor to the ceiling of the cavity. Thin section.

Fig.5 – Marmorito macroconcretion. A) Polished slab of a sample of Marmorito Sandstone crossed by a vein with a complex cement infilling. The squared area indicates location of Fig. 5b. b) Dolomite sphaerulites “float” in a coarse calcite spar. Note that most of them show hollow cores locally with a dumbbell shape (arrows). Thin section. c) Cathodoluminescence image showing the contrast between the finely zoned, greenish yellow dolomite and the orange yellow calcite spar. Thin section. d) Backscattered electron image of the dolomite sphaerulites (dark grey). Note that the cores, locally dumbbell shaped, may be hollow (black) or filled with calcite (light grey). Polished thin section. e) UV epifluorescence image showing the bright colour of the dolomite sphaerulites contrasting with the weak fluorescence of the surrounding calcite spar. Thin section.

Fig.6 - Alfiano Natta macroconcretion. a) Photomosaic of part of the infill of a cm-large fracture (centre of the fracture to the top). Note: the finely laminated fabric with stromatolite-like wavy geometry of the laminae; the occurrence of irregularly shaped or ellipsoidal cement-filled fenestrae. Arrow points to branching microbial laminae. The short and long open arrows point to location of fig. 6d and f respectively. Thin section. b) Close up of an

ellipsoidal fenestra “wrapped” in micritic regular microbial laminae. Thin section. c) UV epifluorescence image of the left-hand part of fig. 6b evidencing the marked fluorescence contrast of the laminae (bright), and the crystalline cement (black). d, e) transmitted light (d) and cathodoluminescence (CL) (e) images of an irregularly shaped fenestra. Note the turbid rim of the walls, dull in CL, that preserves ghosts of pristine fibrous aragonite (arrow); the cavity is plugged with bright orange to brown calcite and very dull limpid dolomite. Thin section. f) Close up of the fenestra indicated with a long arrow in fig. 6a. Note portions of recrystallized aragonite fans rimming the cavity and scattered within calcite spar. Thin section.

Fig.7 - Alfiano Natta macroconcretion. a) General aspect of a sandstone dyke. Note the abundance of muddy matrix among sand grains and the absence of intergranular pores. Thin section. b, c) TL (b) and CL (c) images of a geopetally filled moldic cavity. Note the brightly luminescing finely crystalline dolomite growing within the sediment on the bottom and making a rim at the outer edge, and the dull, limpid sparry dolomite (II+III) filling the upper part of the void. Thin section. d) Backscattered electron image of the sediment in the lower part of the moldic cavity of fig. 7b. The white spots are framboidal pyrite. e, f) TL (e) and CL (f) images of a mud clast cemented by finely crystalline dolomite. Note that crystal size and CL zoning is the same as the lower part of the geopetally-filled moldic pores of Figs. 7b, c).

Fig.8 – Simplified sketch of the step-by-step evolution of pinch out cements. For details see text.

Fig.9 - Simplified sketch of the step-by-step evolution of non gravitational structures. Compare with Fig. 4a. For details see text. (s1 and s2: internal sediments; white area: open space; GH: gas hydrates; c: sparry calcite)

Fig.10 - Simplified sketch of the step-by-step evolution of dolomite crystals floating in calcite spar. For details see text. (Black dots: microbial colonies; S: dolomite sphaerulites; R: dolomite rhombs GH: gas hydrates; M: microbial mat).

Fig.11 - Simplified sketch of the step-by-step evolution of microbial mats. For details see text. . (AR: aragonite fans; GH: gas hydrates; white area: open space; ; M: microbial mat; orange and yellow: sparry cements).

Fig.12 - Simplified sketch of the step-by-step evolution of geopetally filled moldic cavities and dolomite-cemented mud clasts. For details see text. . (Q: quartz; P: plagioclase; S: serpentinite; L: limestone clast; GH: gas hydrates; M: clathrate-cemented mud clast; yellow, orange and brown: subsequent dolomite generations).

Acknowledgments

UV-fluorescence observations were performed at the Plant Biology Department of the Torino University by courtesy of Prof. A. Fusconi. Comments and suggestions by two anonymous referees and the Editor of the journal, B. Jørgensen, greatly improved the text. Research funded by Ministry of University and Research grants (PRIN 2006-07) to P. Clari.

References

Aloisi G, Pierre C, Rouchy J M, Foucher, JP, Woodside J, Party M (2000) Methane-related authigenic carbonates of eastern Mediterranean Sea mud volcanoes and their possible relation to gas hydrate destabilisation. Earth Planet Sci Lett 184:321-338

Arp G, Hofmann J, Reitner J (1998) Microbial Fabric Formation in Spring Mounds ("Microbialites") of Alkaline Salt Lakes in the Badain Jaran Sand Sea, PR China. Palaios 13: 581-592

Beauchamp B (2004) Natural gas hydrates: myths, facts and issues. C. R. Geosci 336: 751–765

Biella G, Polino R, de Franco R, Rossi PM, Clari P, Corsi A, Gelati R (1997) The crustal structure of the Western Po Plain: reconstruction from integrated geological and seismic data. Terra Nova 9:28-31

Bigi G, Cosentino D, Parotto M, Sartori R, Scandone P (1990) Structural model of Italy: Geodinamic project. C.N.R., S.EL.CA, scala 1:500.000, Foglio 1

Boetius A, Ravenschlag K, Schubert C, Rickert D, Gieseke A, Amann R, Widdel F, Jorgensen BB, Witte U, Pfannkuche O (2000) A marine microbial consortium apparently mediating anaerobic oxidation of methane. Nature 407:623-626

Bohrmann G, Greinert J, Suess E, Torres M (1998) Authigenic carbonates from the Cascadia subduction zone and their relation to gas hydrate stability. Geology 26: 647–650

Bohrmann G, Suess E, Greinert J, Teichert B, Naehr T (2002) Gas hydrate carbonates from Hydrate ridge, Cascadia convergent margin: indicators of near-seafloor clathrate deposits. In: Proceedings of the Fourth International Conference on Gas Hydrates, Yokohama, Japan, pp 102-107

Bohrmann G, Torres M (2006) Gas hydrates in marine sediments. In: Schulz HD, Zabel M (Ed) Marine Geochemistry, 2rd edn. Springer pp 481-512

Bojanowski M J (2007) Oligocene cold-seep carbonates from the Carpathians and their inferred relation to gas hydrates. Facies 53:347–360

Brehm U, Krumbein WE, Palinska KA (2006) Biomicrospheres generate ooids in the laboratory. Geomicrobiol Jour 23:545–550

Buczynski C, Chafetz, HS (1991) Habit of bacterially induced precipitates of calcium carbonate and the influence of medium viscosity on mineralogy Jour Sed Petr 61:226–233

Castellarin A (1994) Strutturazione eo- e mesoalpina dell'Appennino settentrionale attorno al nodo ligure: Studi Geologici Camerti, Vol Spec CROP 1-1:99-10

Cavagna S, Clari P, Martire L (1999) The role of bacteria in the formation of cold seep carbonates: geological evidence from Monferrato (Tertiary, NW Italy). Sediment Geol 126:253-270

Chekroun KB, Rodriguez-Navarro C, Gonzalez-Munoz MT, Arias JM, Cultrone G, Rodriguez-Gallego M (2004) Precipitation and growth morphology of calcium carbonate induced by M*yxococcusxanthus*: implications for recognition of bacterial carbonates. Jour Sed Res 74:868-876

Clari P, Cavagna S, Martire L, Hunziker J (2004) A Miocene mud volcano and its plumbing system: a chaotic complex revisited (Monferrato, NW Italy). J Sediment Res 74(5):662–676

Clari P, Dela Pierre F, Martire L, Cavagna S (2009) The Cenozoic CH4-derived carbonates of Monferrato (NW Italy): a solid evidence of fluid circulation in the sedimentary column. Mar Geol, 265:167–184in press

Clari P, Dela Pierre F, Novaretti A, Timpanelli M (1995) Late Oligocene-Miocene sedimentary evolution of the critical Alps-Apennines junction: the Monferrato area, Northwestern Italy. Terra Nova 7:144-152

Clari P, Fornara L, Ricci, Zuppi GM (1994) Methane-derived carbonates and chemosymbiotic communities of Piedmont (Miocene), Northern Italy: an update. Geo-Mar Lett 14:201–209

Clari P, Gagliardi C, Governa ME, Ricci B, Zuppi GM (1988) I calcari di Marmorito: una testimonianza di processi diagenetici in presenta di metano. Boll Mus Reg Sci Nat Torino, 6(1):197-216

Clari P, Ghibaudo G (1979) Multiple slump scars in the Tortonian type area – Piemont Basin, North-Western Italy. Sedimentology 26:719-730

Clari P, Martire L (2000) Cold seep carbonates in the Tertiary of Northwestern Italy: evidence of bacterial degradation of methane. In: Riding RE & Awramik SM (Eds) Microbial sediments, Springer-Verlag, Heidelberg, pp 261-269

Clari P., Martire L. (1995). I calcari metano-derivati del Monferrato: caratteristiche petrografiche e possibile significato geologico. In: R. Polino and R. Sacchi (Eds.), Atti Convegno Rapporti Alpi-Appennino, Peveragno 31 maggio-1 giugno 1994. Acc. Naz. Sci. detta dei XL, Scritti e documenti 14, Roma: 21-37

Collett TS (2002) Energy resource potential of natural gas hydrates. AAPG Bull 86:1971–1992

Dählmann A, de Lange GJ (2003) Fluid-sediment interactions at eastern Mediterranean mud volcanoes: a stable isotope study from ODP Leg 160. Earth Planet Sci Lett 212:377–391

Dalla S, Rossi M, Orlando M, Visentin C, Gelati R, Gnaccolini M, Papani G, Belli A, Biffi U, Catrullo D (1992) Late Eocene-Tortonian tectono-sedimentary evolution in the western part of the Padan Basta (Northern Italy): Paleontol y Evol 24-25:341-362

Dela Pierre F, Clari P, Cavagna S, Bicchi E (2002) The Parona chaotic complex: a puzzling record of the Messinian (Late Miocene) events in Monferrato (NW Italy). Sediment Geol 152:289-311

Dela Pierre F, Festa A, Irace A (2007) Interaction of tectonic, sedimentary, and diapiric processes in the origin of chaotic sediments: An example from the Messinian of Torino Hill (Tertiary Piedmont Basin, northwestern Italy). Geol Soc Am Bull 119:1107-1119

Dela Pierre F, Martire L, Natalicchio M, Clari P, Petrea C (2009) Authigenic carbonates in Upper Miocene sediments of the Tertiary Piedmont Basin (NW Italy): Vestiges of an ancient gas hydrate stability zone? Geol Soc Am Bull, in press

Dela Pierre F, Piana F, Fioraso G, Boano P, Bicechi E, Forno MG, Violanti D, Clari P, Polino R, (2003) Note Illustrative della Carta Geologica d'Italia alla scala 1:50.000. Foglio 157 "Trino". Litografia Geda, Nichelino (To), pp 147

Dewhurst DN, Cartwright JA, Lonergan L (1999) The development of polygonal fault systems by syneresis of colloidal sediments. Mar and Petrol Geol 16:. 793–810

Dickens GR (2003) Rethinking the global carbon cycle with a large, dynamic and microbially mediated gas hydrate capacitar. Earth Planet Sci Lett 213:169-183

Elter P, Pertusati P (1973) Considerazioni sul limite Alpi-Appennino e sulle relazioni con l'arco delle Alpi occidentali. Mem Soc Geol Ital 12:359-375

Falletti P, Gelati R, Rogledi S (1995) Oligo-Miocene evolution of Monferrato and Langhe, related to deep structures. In: Polino R, Sacchi R (Eds) Atti del Convegno Rapporti Alpi-Appennino: Accad Naz Sci detta dei XL, Scritti e Documenti 14:1-19

Fernandez Diaz L, Putnis A, PrietoM, Putnis CV (1996) The role of magnesium in the crystallization of calcite and aragonite in a porous medium. Jour Sed Res 66:482-491

Gelati R, Gnaccolini M (1988) Sequenze deposizionali in un bacino episuturale, nella zona di raccordo tra Alpi ed Appennino settentrionale: Atti Ticin Sci Terra 31:340-350

Ghibaudo G, Clari P, Perello M (1985) Litostratigrafia, sedimentologia ed evoluzione tettonico- sedimentaria dei depositi miocenici del margine Sud- Orientale del Bacino Terziario Ligure-Piemontese (Valli Borbera, Scrivia e Lemme): Boll Soc Geol Ital 104:349-397

Gomez-Perez I (2003) An Early Jurassic deep-water stromatolitic bioherm related to possible methane seepage (Los Molles Formation, Neuquen, Argentina). Palaeogeogr Palaeoclimat Palaeoecol 201:21-49

Greinert J, Bohrmann G, Suess E (2001) Gas hydrate-associated carbonates and methane-venting at Hydrate Ridge: classification, distribution, and origin of authigenic lithologies. In: Paull CK, Dillon WP (Eds), Natural Gas Hydrates: Occurrence, Distribution, and Detection, American Geophysical Union, Washington, DC:99–113

Haq BU (1993) Deep-sea response to eustatic change and significance of gas hydrates for Continental margin stratigraphy. International Association of Sedimentologists, Spec Publ 18:93-106

Hendry JP, Pearson MJ, Trewin NH, Fallick AE (2006) Jurassic septarian concretions from NW Scotland record interdependent bacterial, physical and chemical processes of marine mudrock diagenesis. Sedimentology: 53: 537–565

Krause FF (2001) Genesis and geometry of the Meiklejohn Peak lime mud-mound, Bare Mountain Quadrangle, Nevada, USA: Ordovician limestone with submarine frost heave structures-a possible response to gas clathrate hydrate evolution. Sediment Geol 145:189-213

Kvenvolden KA (1998) A primer on the geological occurrence of gas hydrate. In: Henriet JP. & Mienert J (eds) Gas hydrates: Relevance to world margin stability and climate change. Geol Soc Lond Spec Publ 137:9-30

Liu X, Flemings PB (2006) Passing gas through the hydrate stability zone at southern Hydrate Ridge, offshore Oregon. Earth and Planetary Science Letters, 241: 211-226

Mazzini A, Svensen H, Hovland M, Planke S (2006) Comparison and implications from strikingly different authigenic carbonates in a Nyegga complex pockmark, G11, Norwegian Sea. Mar Geol 231:89–102

Mc Crea JM (1950) The isotopic chemistry of carbonates and a paleotemperature scale. J Chem Phys 18:849

Meister P, Bernasconi S M, Vasconcelos C, McKenzie JA (2008) Sealevel changes control diagenetic dolomite formation in hemipelagic sediments of the Peru Margin. Mar Geol 252:166-173

Meister P, McKenzie JA, Vasconcelos C, Bernasconi S, Frank M, Gutjahr M, Schrag DP (2007) Dolomite formation in the dynamic deep biosphere, results from the Peru Margin, OPD Leg 201. Sedimentology 54:1007–1032

Mienert J, Posewang J, Baumann M (1998). Gas hydrates along the north-eastern Atlantic Margin: possible hydrate bound margin instabilities and possible release of methane. In: Henriet JP. & Mienert J (eds) Gas hydrates: Relevance to world margin stability and climate change. Geol Soc Lond Spec Publ 137:275–291

Mienert J, Vanneste M, Bünz S, Andreassen K, Haflidason H, Sejrup HP (2005) Ocean warming and gas hydrate stability on the mid-Norwegian margin at the Storegga Slide. Mar Petrol Geol 22:233–244

Milkov AV (2004) Global estimates of hydrate-bound gas in marine sediments: how much is really out there? Earth-Sci Rev 66:183–197

Mutti E, Papani L, Di Biase D, Davoli G, Segadelli S, Tinterri R (1995) II Bacino Terziario Epimesoalpino e le sue implicazioni sui rapporti Alpi-Appennino. Mem Sci Geol 47:217-244

Pache M, Reitner J, Arp G (2001) Geochemical evidence for the formation of a large Miocene "travertine" mound at a sublacustrine spring in a soda lake (Wallerstein Castle Rock, Nordlinger Ries, Germany). Facies 45:211-230

Paull CK, Buelow WJ, Ussler W, Borowski WS (1996) Increased continental-margin slumping frequency during sea-level lowstands above gas hydrate-bearing sediments. Geology 24:143-146

Pecher IA, Kukowski N, Huebscher C, Greinert J, Bialas J and the GEOPECO Working Group (2001) The link between bottom-simulating refections and methane flux into the gas hydrate stability zone - new evidence from Lima Basin, Peru Margin. Earth Planet Sci Lett 185:343-354

Piana F (2000) Structural setting of Western Monferrato (Alps-Apennines Junction Zone, NW Italy). Tectonics 19:943-960

Piana F, Polino R (1995) Tertiary structural relationships between Alps and Apennines - the critical Torino Hill and Monferrato area, northwestern Italy. Terra Nova 7:138-143

Pierre C, Rouchy JM (2004) Isotopic compositions of diagenetic dolomites in the Tortonian marls of the western Mediterranean margins: evidence of past gas hydrate formation and dissociation. Chem Geol 205:469– 484

Pierre C, Rouchy JM, Blanc-Valleron MM (2002) Gas hydrate dissociation in the Lorca Basin (SE Spain) during the Mediterranean Messinian salinity crisis. Sediment Geol 147:247-252

Pini GA (1999) Tectonosomes and Olistostromes in the Argille Scagliose of the Northern Apennines, Italy. Geol Soc Am Spec Paper 335:73

Ramsay JG (1980) The crack-seal mechanism of rock deformation. Nature 284:135-139

Reid RP, Visscher PT, Decho AW, Stolz JF, Bebout BM, Dupraz C, Macintyre IG, Paerl HW, Pinckney JL, Prufert-Bebout L, Steppe TF, DesMarais DJ (2000) The role of microbes in accretion, lamination and early lithification of modern marine stromatolites. Nature 406:989-992

Reitner J, Peckmann J, Reimer A, Schumann G, Thiel V (2005) Methane-derived carbonate build- ups and associated microbiai communities at cold seeps on the lower Crimean shelf (Black Sea). Facies 51:66-79

Roure F, Bergerat F, Damotte B, Mugnier JL Polino R (1996) The Ecors-Crop Alpine seismic traverse. Bull Soc Geol Fr 170:1-113

Sain K, Minshull TA, Singh SC, Hobbs RW (2000) Evidence for a thick free gas layer beneath the bottom simulating reflector in the Makran accretionary prism. Mar Geol 164:3–12

Solomon EA, Kastner M, Jannasch H, Robertson G, Weinstein Y (2008) Dynamic fluid flow and chemical fluxes associated with a seafloor gas hydrate deposit on the northern Gulf of Mexico slope. Earth Planet Sci Lett 270:95-105

Teichert B, Gussone N, Eisenhauer A, Bohrmann G (2005) Clathrites: Archives of near-seafloor pore-fluid evolution (δ 44/40Ca, δ 13C, δ 18O) in gas hydrate environments. Geology 33(3):213-216

Tracy SL, Williams DA, Jennings HM (1998) The growth of calcite spherulites from solution II. Kinetics of formation: Jour Crystal Growth 193:382–388

Warren LA, Maurice, PA, Parmar N, Ferris FG (2001) Microbially mediated calcium carbonate precipitation: implications for interpreting calcite precipitation and for solid phase capture of inorganic contaminants Geomicrobiol Jour 18:93–115

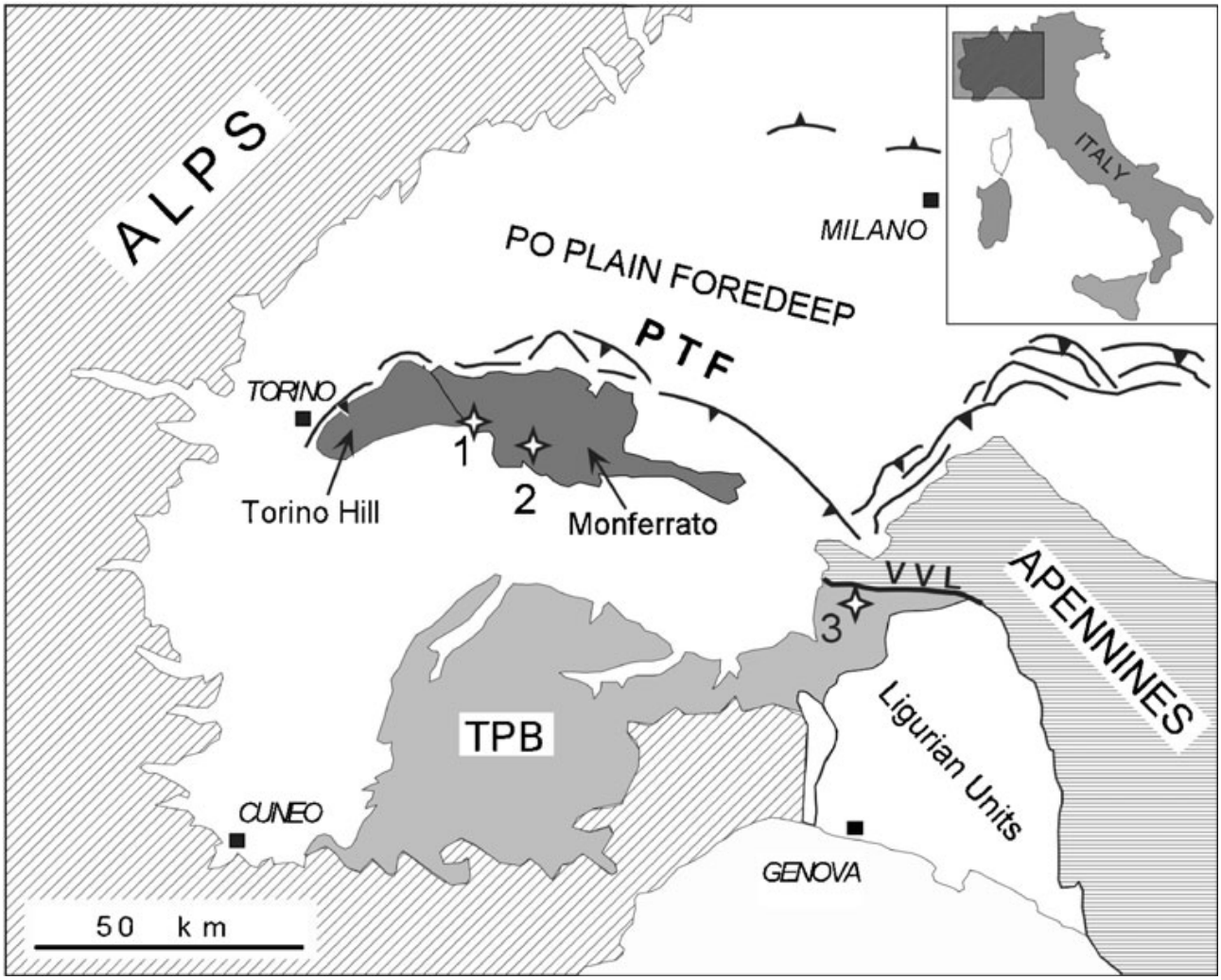
ALPS
PO PLAIN FOREDEEP
PTF
MILANO
ITALY
TORINO
1
2
Torino Hill
Monferrato
VVL
3
APENNINES
TPB
Ligurian Units
CUNEO
GENOVA
50 km

Fig. 1

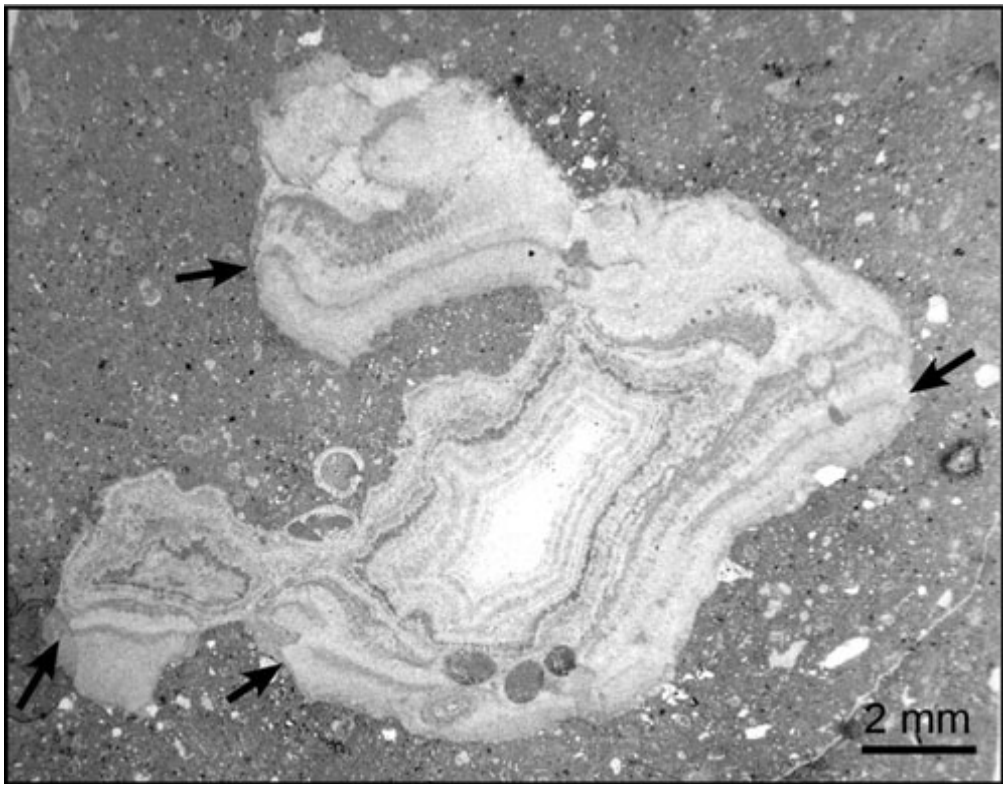

Fig. 2

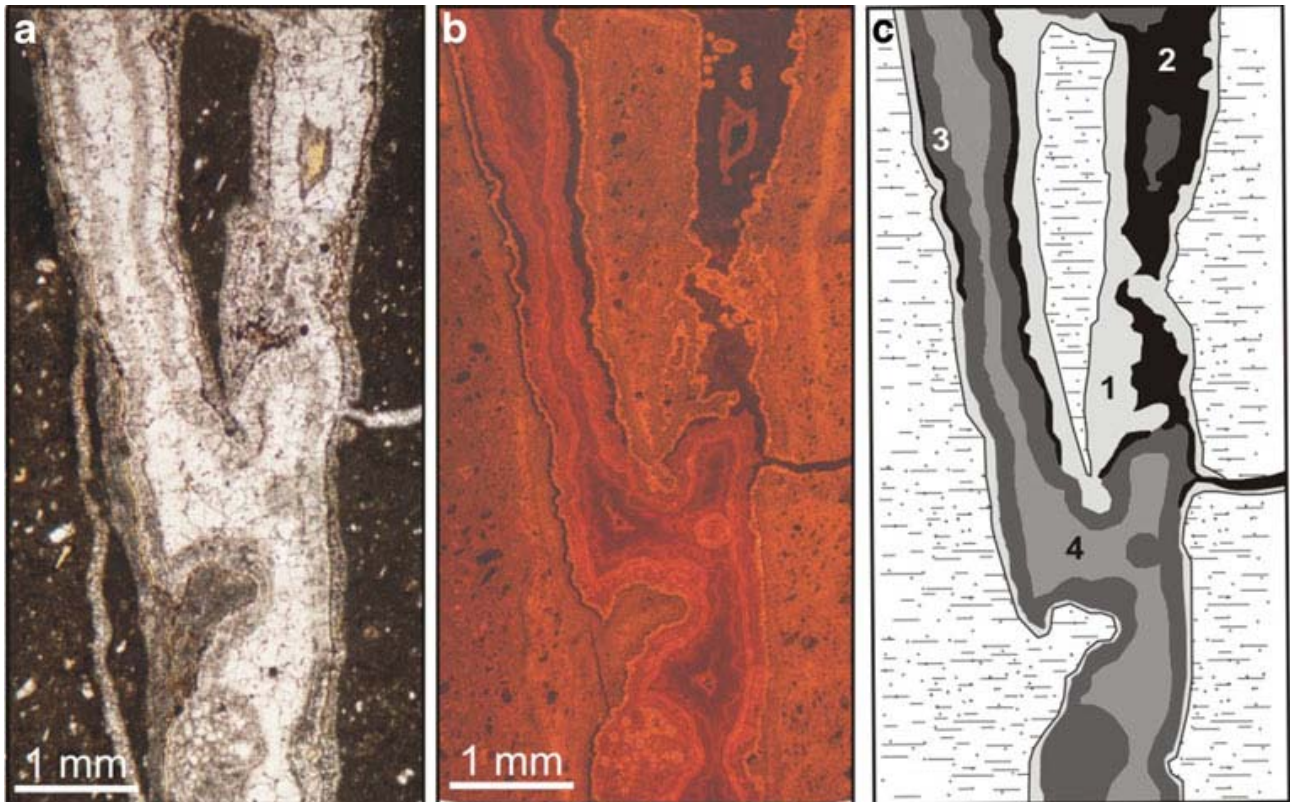

Fig. 3

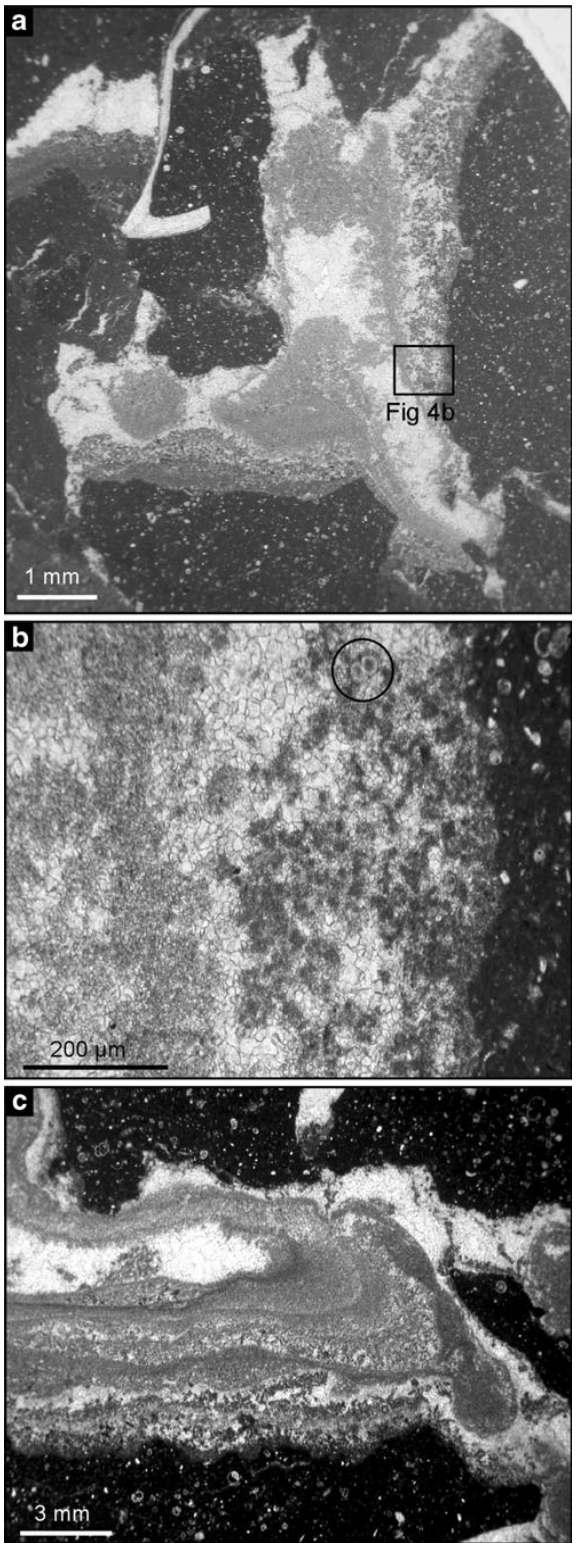

Fig. 4

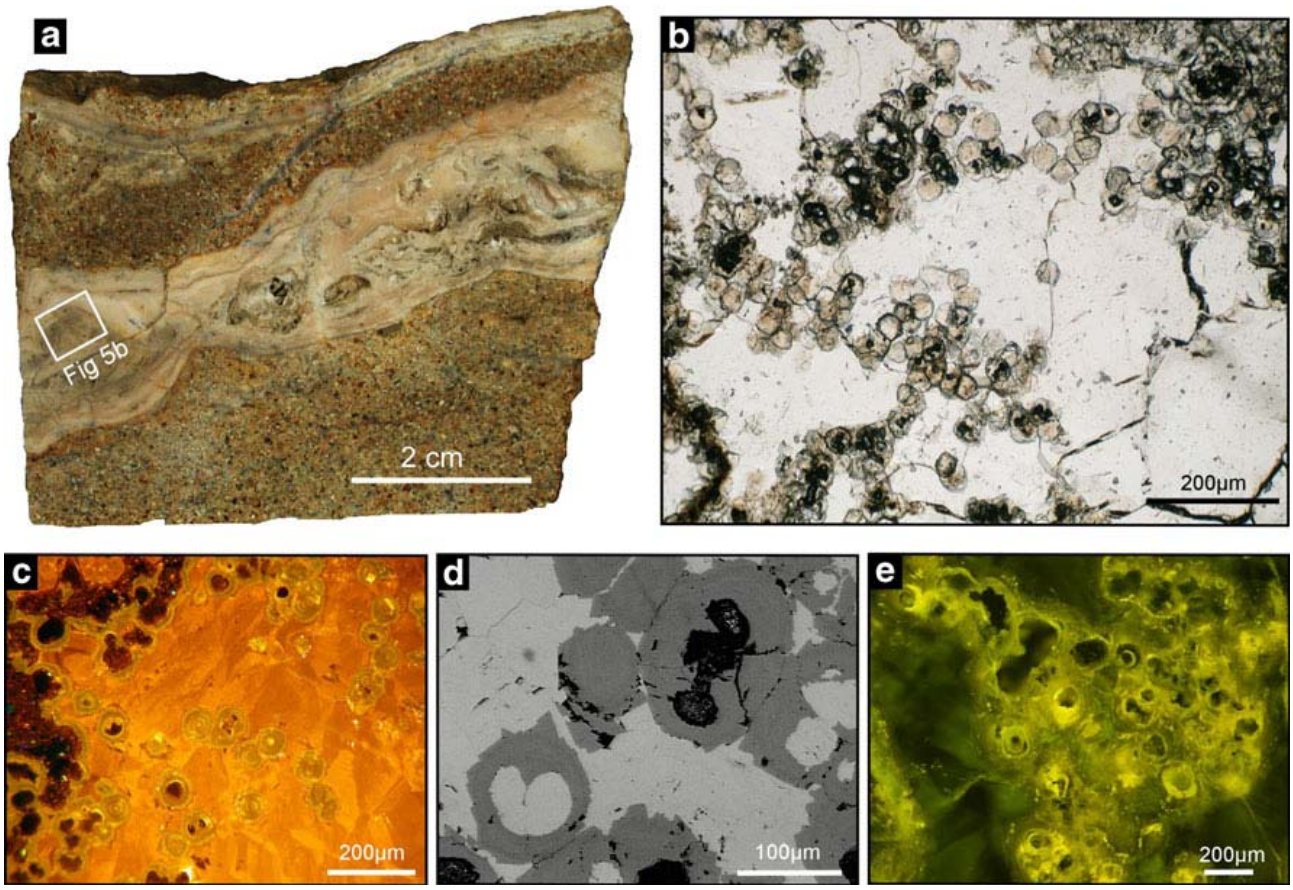

Fig. 5

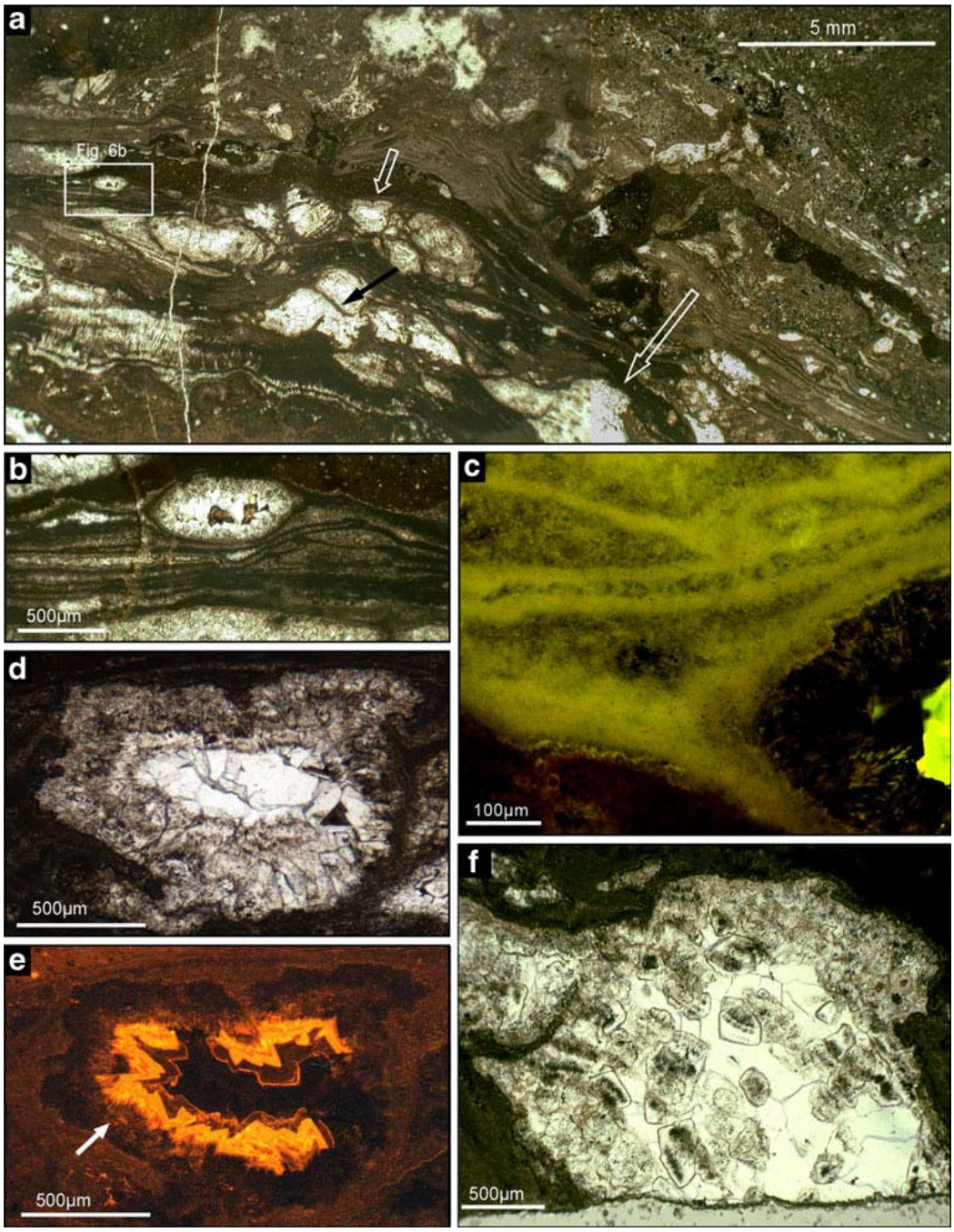

Fig. 6

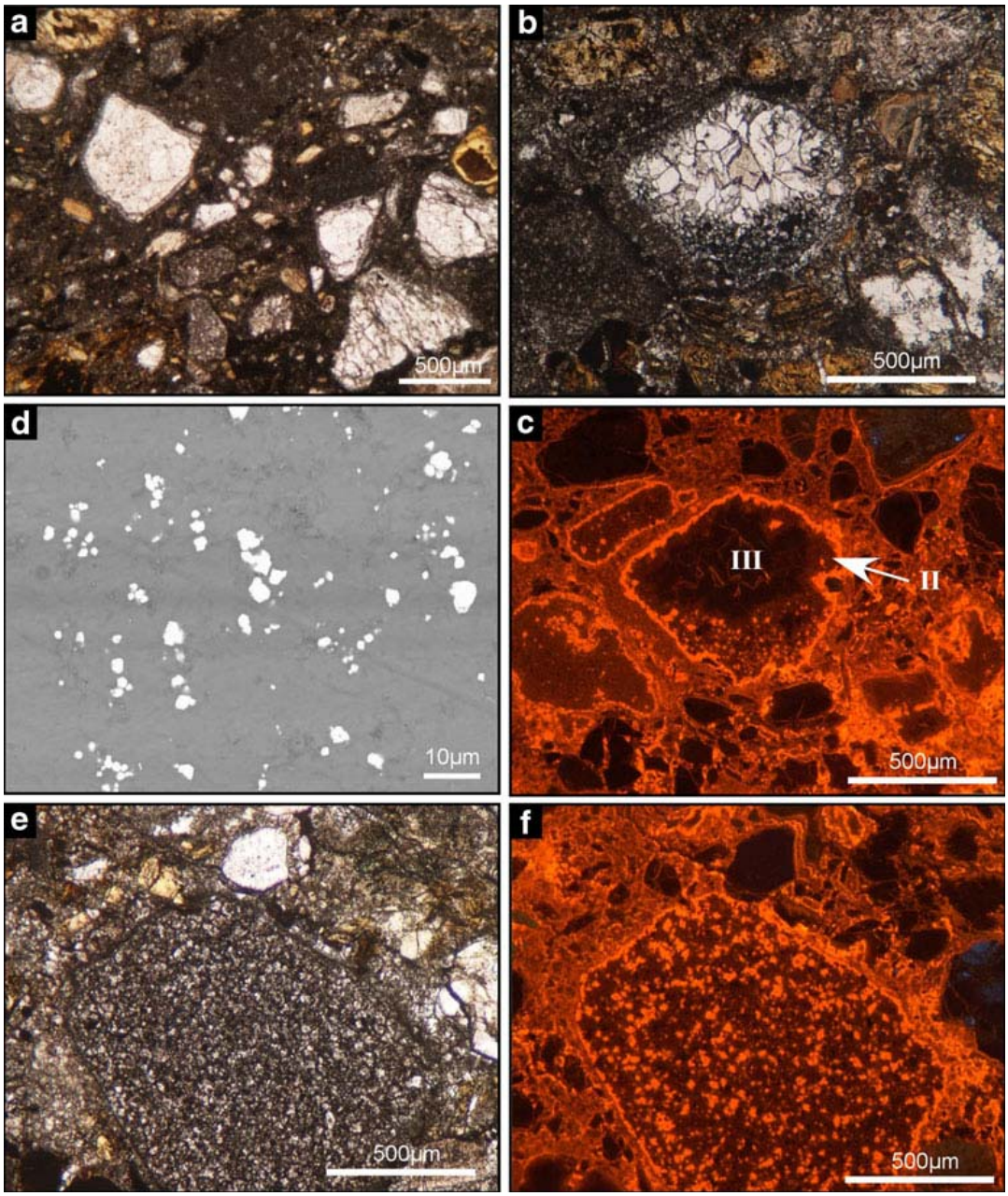

Fig. 7

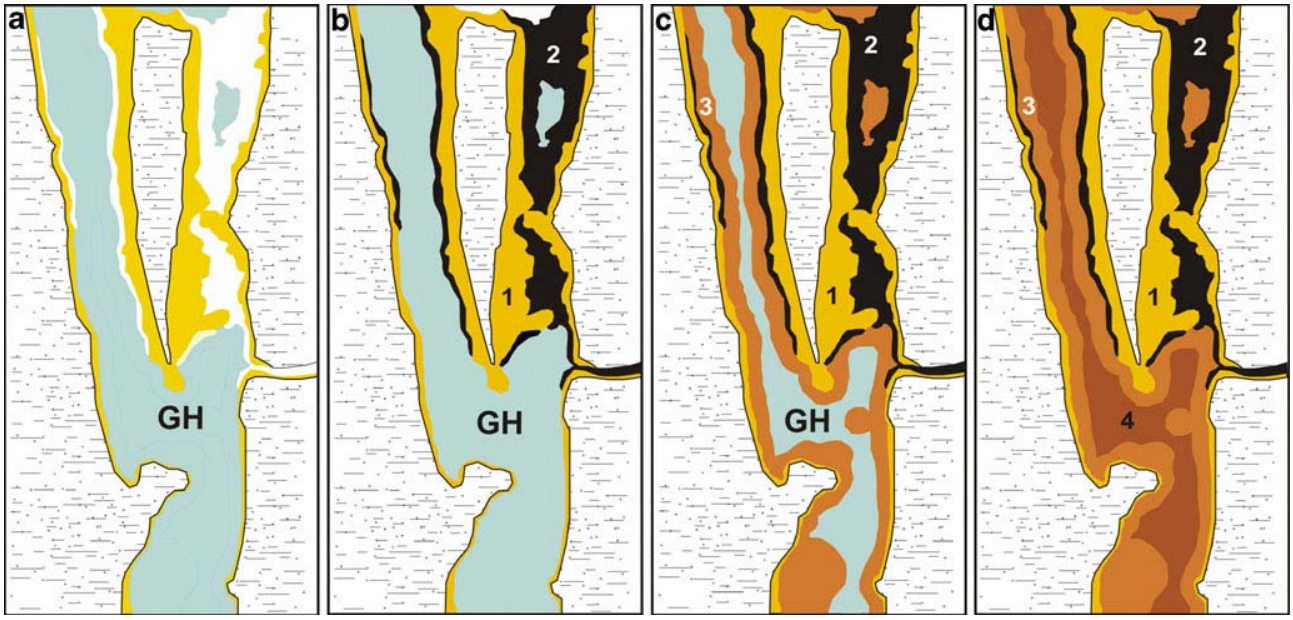

Fig. 8

Fig. 9

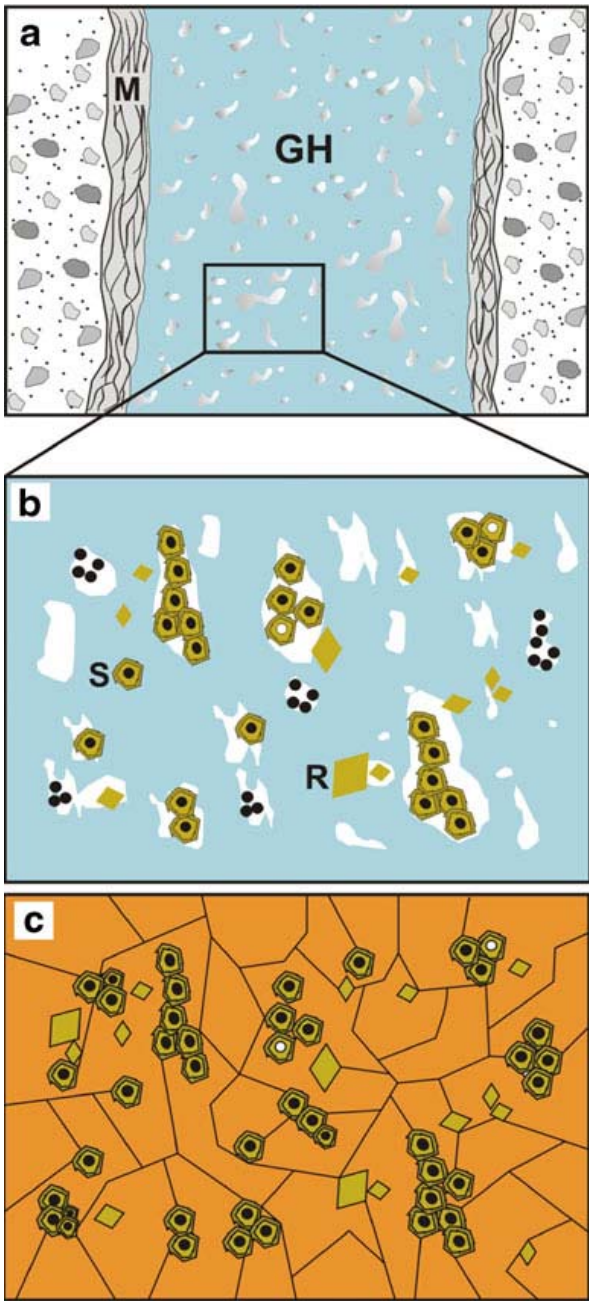

Fig. 10

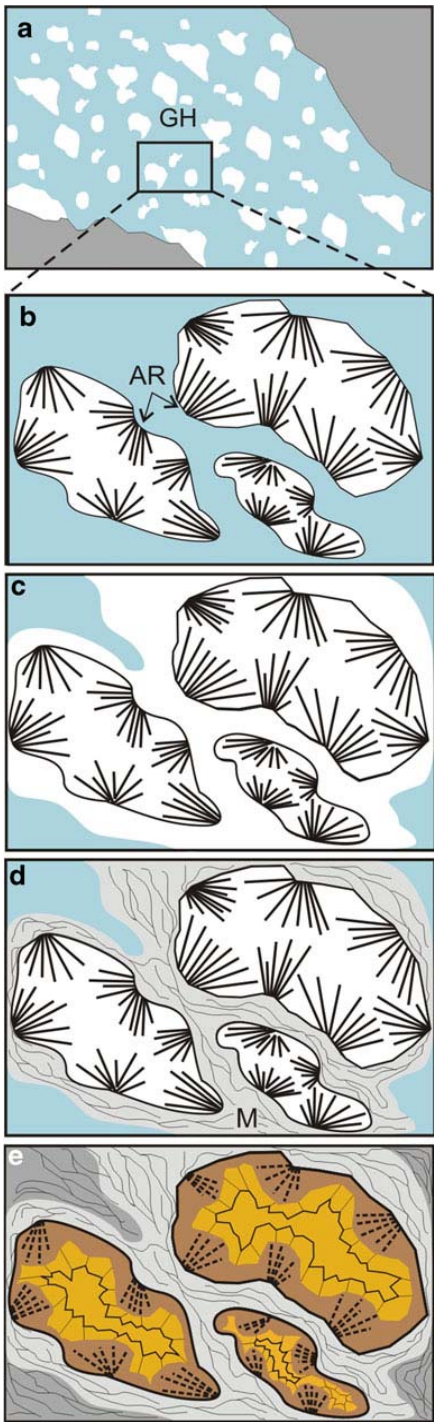

Fig. 11

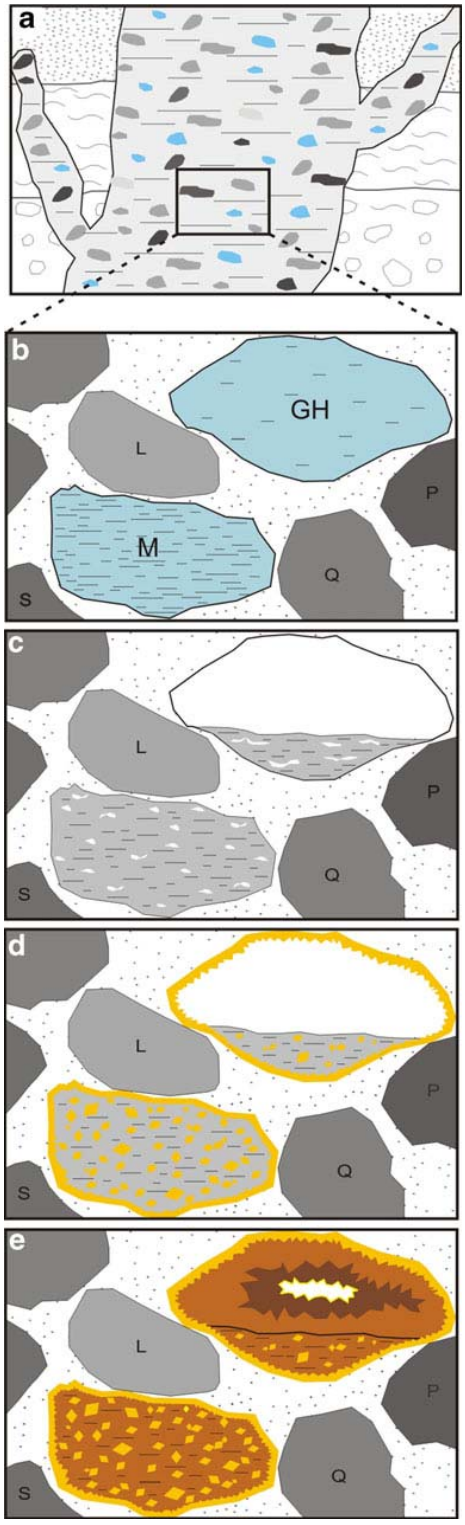

Fig. 12